20 KSME International Journal, Vol. 11, No. 1, pp. 20~28, 1997

Experimental Investigations of Sideward Burr Formation in Rotary Machining

Gi Heung Choi*

(*Received January 17, 1996*)

Burrs can be formed on the feed mark ridges and the edges of the machined parts in machining operations. These burrs are undesirable in terms of the surface quality, the precise dimensioning of the machined parts and the safety of operators. This paper demonstrates the effectiveness of using a rotary tool on minimizing the sideward burr formation in machining. In particular, the experimental relationships between the size of sideward burr and the cutting parameters (including tooling mechanism) are established first in rotary machining. Methods to control the size of sideward burr are then explained. The possible application of a rotary tool for deburring operations while engaged in machining is also explored.

Key Words: Sideward Burr, Poisson Burr, Rotary Machining

Nomenclature

F_c : Cutting force component in the cutting speed direction
F_l : Cutting force component along the cutting edge
F_x : Cutting force components in x direction
F_y : Cutting force components in y direction
H_P : Height of Poisson burr
H_S : Height of sideward burr
H_{yo} : $H_S - H_P$
i_F : Oblique angle
i_{eq} : Equivalent oblique angle
l : Length of workpiece
t_1 : Depth of cut
V_t : Tool velocity
V_w : Cutting velocity (speed)
w : Width of cut
α_n : Normal rake angle
α_g : Geometric rake angle
ϕ_n : Normal shear angle
η_c : Chip flow angle
θ_h : Tool setting angle
θ_v : Tool setting angle

* Department of Industrial Safety Engineering, Hansung University, 389 Samsun-dong 2-ga, Sungbuk-gu, Seoul, Korea (136-792)

1. Introduction

Burrs produced on the surfaces or on the edges of the machined parts are undesirable in terms of the surface quality, effective functioning and precise dimensioning of the machined parts, and the safety of operators. In some cases, burrs can cause the rubbing wear of the tool during the machining (Pekelharing and Gieszen, 1971). These burrs must be completely removed in most cases. One way of removing burrs left on the machined surface is the polishing operation. Also the burrs left on the edges of the machined parts can be removed by deburring operation. These approaches are, however, highly costly since considerable amount of time and effort are needed as the production increases. Formation of burrs in machining can also be minimized by properly selecting the cutting parameters and workpieces. However, this causes some limitations on the productivity and the automation of the production.

Burrs can be conveniently classified into four types depending on the location where they develop (Nakayama and Arai, 1987) : backward (entrance) burr by backward flow of materials,

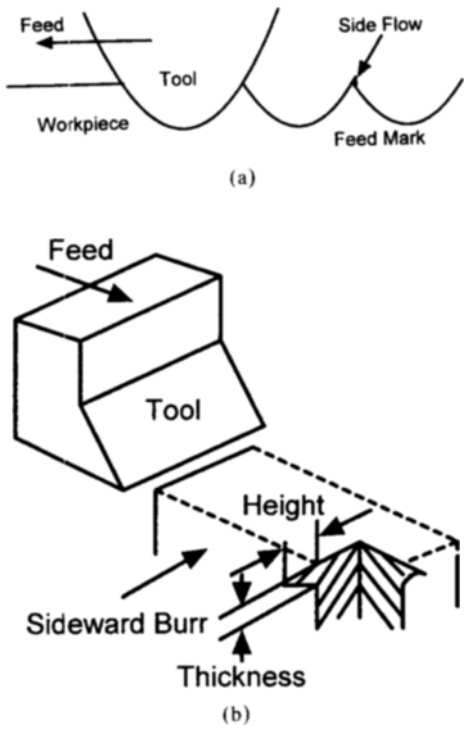

Fig. 1 Typical sideward burr formed in single point cutting, (a) and in orthogonal cutting, (b).

sideward burr by sideward flow, forward (exit) burr by forward flow and leaned burr by leaning to the feed direction. Figure 1(a) and 1(b) show the typical sideward burr formed in single point turning and in orthogonal cutting, respectively. Depending on the mechanism of formation, there are four basic types of burrs (Gillespie and Blotter, 1976) : Poisson burr, rollover burr, tear burr and cut-off burr. Although some burrs can be a combination of these burrs, one mode of formation usually predominates. The Poisson burr is the result of a material's tendency to bulge at the sides when it is compressed. The rollover burr is essentially a chip which is pushed out of the cutter's path rather than sheared. It is usually found at the end of cut.

It has been well known for some years that burrs formed on the feed mark ridges are caused by the material side flow, i.e., the displacement of work material opposite to the feed direction or movement of material in a direction perpendicular to the direction of cutting. The material side flow is known to be caused by the squeezing effect that the material is pressed sideways where it could escape. Such effect is due to the local pressure between the flank surface of the tool and the workpiece surface being generated. One supporting evidence for this hypothesis is that the squeezing effect is more pronounced with a worn tool than with a fresh tool (Pekelharing and Gieszen, 1971). Consequently, pressure distribution around the tool tip which depends on both the chip formation process and the tool condition appears to be a key factor in minimizing the material side flow.

The main purpose of this study is to demonstrate the effectiveness of using a rotary tool for achieving precision by minimizing the sideward burr formation. Apparently, no attention has ever been paid to the investigation of the sideward burr formation and its removal in rotary machining. In particular, the experimental relationships between the size of sideward burr and the cutting parameters (including the tooling mechanism) are established first in rotary machining. Methods to control the size of sideward burr are then explained. The possible application of the rotary tool for deburring operations while engaged in machining is also explored. Only Poisson burr and rollover burr are considered in this study.

2. Burr Formation in Rotary Machining

The primary design specifications for a long tool life in conventional single point cutting are such that the cutting tool is designed to meet the conditions of minimum total energy (shear and frictional), and reasonable strength and thermal capacity. However, the problem noted in practice is that these conditions are mutually dependent so that only a compromise solution is possible (Shaw, et al, 1952). For example, cutting tools that can insure a reasonable performance and a long tool life must have:

1. both a large effective rake angle (for shear process) and a small actual rake angle (for strength and heat flow),

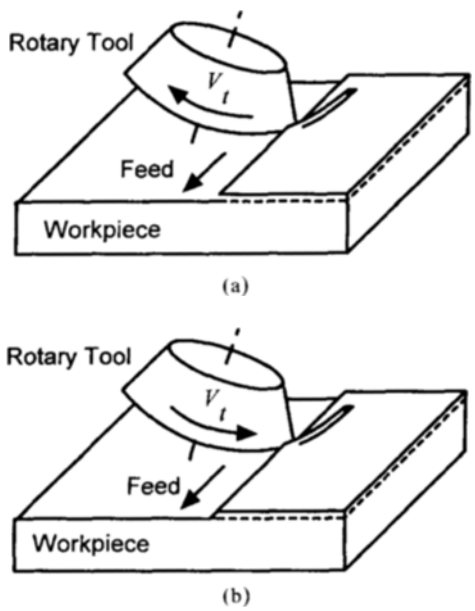

Fig. 2 Normal rotation, (a), and reverse rotation, (b), of a rotary tool.

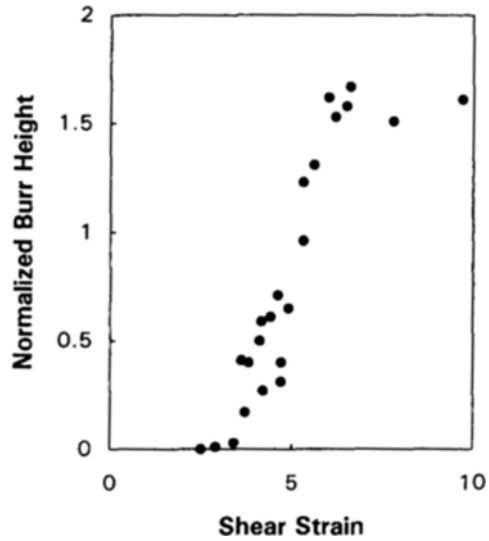

Fig. 3 Experimental relation between the normalized burr height (burr height/depth of cut) and the shear strain obtained in machining 35~65 brass (Nakayama and Arai, 1987).

2. the possibility of increasing the chip velocity without increasing the cutting speed, and

3. positive means for carrying the cutting fluid to the cutting point at the high cutting speed.

Such requirements can be met simply by introducing the additional tool motion parallel to the cutting edge while the workpiece approaches the cutting edge. One way of achieving this tool motion in a continuous fashion is to use a rotary tool which has a circular disc shape. The rotary motion of the tool brings about an intermittent contact between the cutting area of the tool and the workpiece. The typical advantages of rotary tool cutting over the conventional single point cutting are longer tool life, better surface finish and easier control of chip formation process.

The tool can be driven either by the external drive (driven rotary tool, DRT) or by the rolling action with the workpiece (self propelled rotary tool, SPRT). When the projection of the direction of the rotation of cutting edge in the contact zone into the cutting speed direction is along or against the cutting speed vector, it is defined as the normal rotation or the reverse rotation as shown in Figs. 2(a) and 2(b), respectively.

In rotary machining, the level of pressure around the tool tip can be controlled simply by adjusting the rotary speed ratio V_t/V_w. This makes the in-process control of the material side flow realizable in practice. As for burrs on the edge, a unique relationship between the normalized burr height (burr height divided by the depth of cut) and the shear strain was observed while machining 65-35 brass as shown in Fig. 3 (Nakayama and Arai, 1987). In that study, the size of burr was found to depend on the shear strain only. In general, the shear strain (γ) is related to the normal shear angle (ϕ_n) by

$$\gamma = \cot\phi_n + \tan(\phi_n - \alpha_n) \tag{1}$$

Then, ϕ_n is a key factor controlling the size of burr in this case. It is often noted that when machining with a DRT at high rotary speed ratio (V_t/V_w), the tool is unable to carry the chip with it so that significant sliding occurs at the tool-chip interface. As a result, the friction condition is eased and the normal shear angle increases drastically as shown in Fig. 4. Such experimental results strongly suggest that a high rotary speed

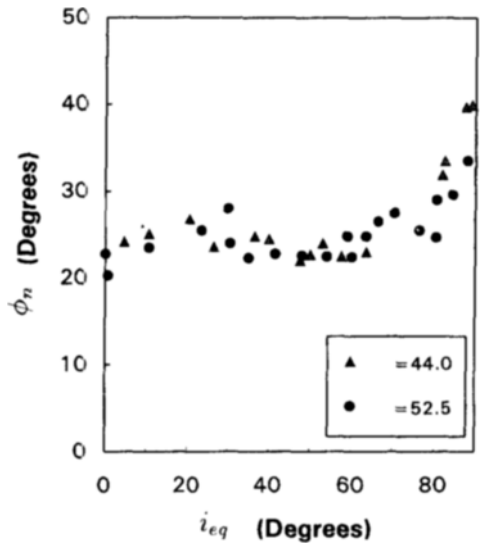

Fig. 4 Variation of ϕ_n with i_{eq} in rotary machining (Venuvinod, 1970).

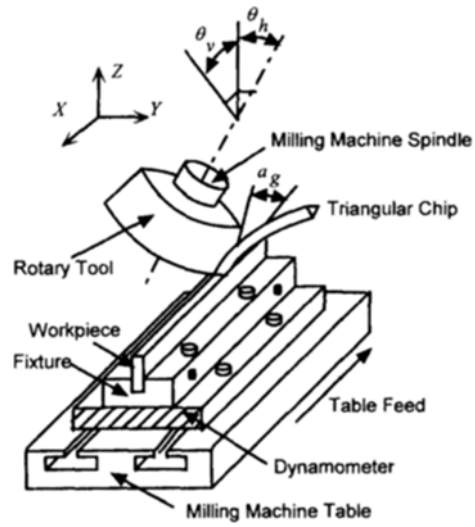

Fig. 5 Experimental setup used in this study.

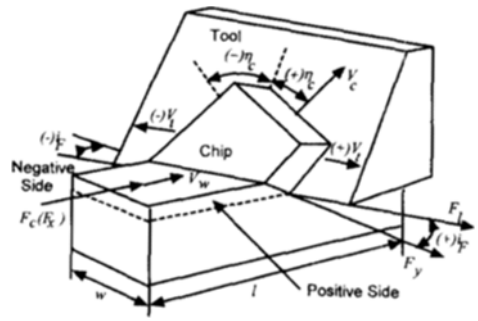

Fig. 6 Designation of angles and velocities in three dimensional cutting

ratio can insure a minimum level of burr formation on the edges of the parts being machined. The equivalent oblique angle i_{eq} in Fig. 4 is distinguished from the static obliquity i_F in that it signifies the angle formed by the relative velocity between the workpiece and the rotary tool, and is given by (Venuvinod, 1970, and Venuvinod and Lau, 1981)

$$i_{eq}=i_F+\tan^{-1}\left(\frac{V_t\cos i_F}{V_w+V_t\sin i_F}\right) \tag{2}$$

3. Experiments

A series of tests were conducted at low cutting speed on a Bridgeport vertical milling machine. The flat workpieces used were $6.35mm$ wide and $45.7mm$ long. Figure 5 illustrate the experimental setup used. Workpieces were mounted on a Kistler 9270A three component dynamometer using a specially designed fixture. The dynamometer was then mounted on the milling machine table. HSS rotary tools with grade M2 and hardness RC65 were mounted on the spindle unit of the milling machine. Tool diameter was $40mm$ and no lubricant was used. These tools can rotate freely when allowed to roll with the workpiece (SPRT). When powered by the spindle unit the tool becomes a DRT. A relationship between the setting angles (θ_h and θ_v) and i_F, and another relationship between these angles and the normal rake angle α_n at the deepest point of penetration of the cutting edge into the workpiece are given by (Venuvinod, 1970)

$$\tan i_F=\frac{\sin i\theta_h}{\tan\theta_v} \tag{3}$$

$$\alpha_n=\alpha_g-\cos^{-1}(\cos\theta_h\cos\theta_v)$$

where α_g is the geometric rake angle of the tool. The size of burr was measured using a micrometer at three different locations after the initial transient period of burr formation stabilized to the steady state condition. Such stabilization typically

took place after the tool traveled approximately 30mm from its initial contact with the workpiece. The cutting force components measured were directly coupled to a strip chart recorder. Since the thickness of burr in Fig. 1(b) for varying cutting parameters exhibits a similar trend as the height (Nakayama and Arai, 1987). only the height of sideward burr is considered in this study. Hereafter, the size of burr implies the height of burr. Figure 6 depicts the ideal three dimensional cutting where angles and velocities are designated. The negative values of burr height represent the burrs on the negative side of the workpiece.

4. Results and Discussions

It was observed during the experiments that linear relationships between the height of Poisson burr(H_P) and the depth of cut hold for various workpieces,i_F and tooling mechanisms. Note that the cutting force component along the tool cutting edge (F_i) is negligible and the cutting force component in the cutting speed direction($F_x = F_c$) is proportional to depth of cut in orthogonal cutting, i.e.,

$$F_x = K_1 t_1 + K_2 \quad (4)$$

where K_1 is the proportionality constant. K_2 is the intercept value obtained from the force-depth of cut plot. Similarly, experimental data in Fig. 7 suggest a linear relationship between F_x and H_P such that

$$H_P = C_1 F_x + C_2 \quad (5)$$

It may also be stated from the results in Fig. 7 that the ductility of Al1100 is mostly responsible

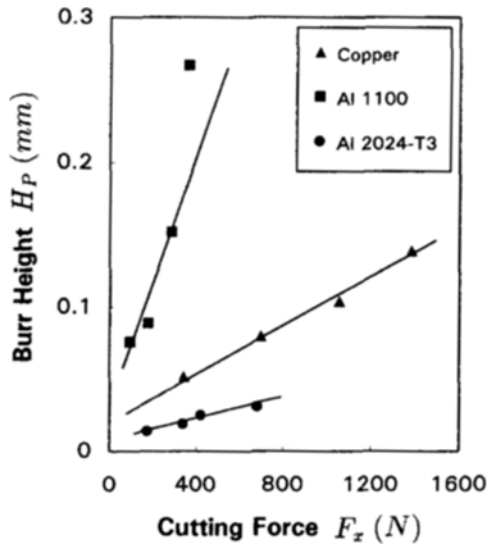

Fig. 7 Variation of H_P with F_x in orthogonal cutting. Cutting conditions are : V_w=0.3 m/min, t_1=0.051~0.203 mm and α_n=10°.

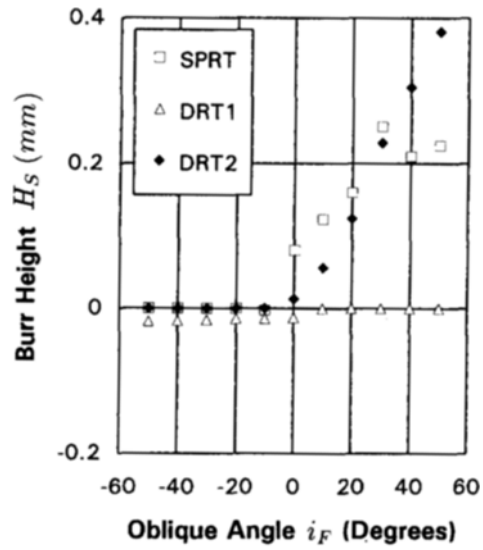

(a)

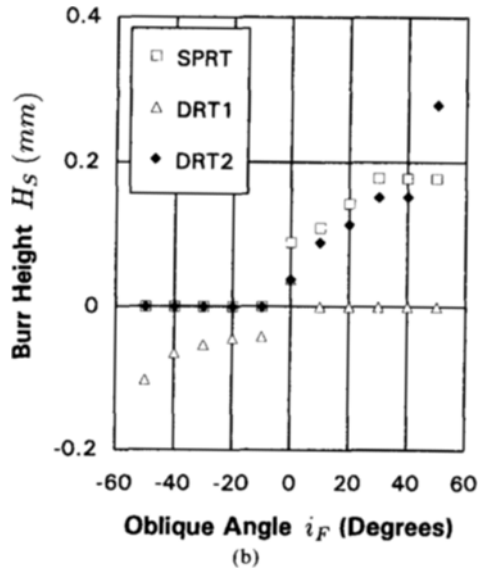

(b)

(Fig. 8 Continued)

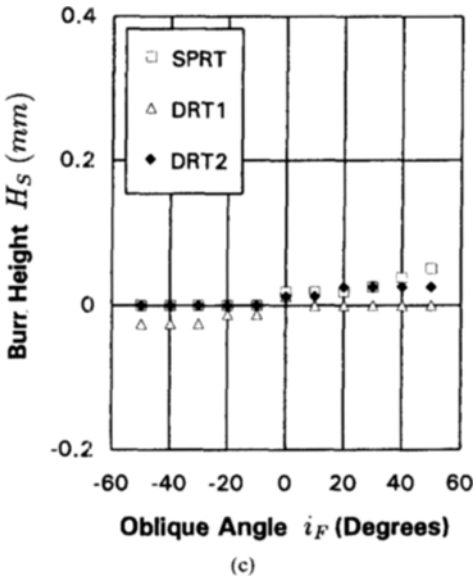

(c)

Fig. 8 Variation of H_S with i_F. Workpiece: Copper, (a); Al1100, (b); Al2024~T3, (c). Cutting conditions are same as in Fig. 7.

for the larger size of Poisson burr since the ductile materials can sustain larger plastic deformation, whereas the brittle materials such as A1204-T3 have very little capacity for plastic deformation (Ko, 1989, and Choi, 1990).

Figure 8 shows the variation of the height of sideward burr (H_S) with the oblique angle i_F for workpieces, cutting conditions and tooling mechanisms indicated. Machining with a SPRT revealed a trend that the larger size of burr is formed on the positive side of the workpiece than on the negative side. However, it was observed during the experiments with a driven rotary tool at high rotary speed ratio in reverse rotation ($V_t/V_w=-6.7/0.3$ hereafter DRT1) that the size of burr was rather larger on the negative side of the workpiece. In this case, i_{eq} is less than $-70°$ for all i_F tested and the chip flow was always in the negative direction ($\eta_c<0$). Furthermore, the maximum size of burr was obtained for a driven rotary tool at high speed ratio in normal rotation ($V_t/V_w=6.7/0.3$ and $i_{eq}>70°$ for all i_F tested, hereafter DRT2) where the chip flow angle is maximum in the positive direction ($\eta_c\approx 90°$) These observations strongly suggest that

1. there exists a strong correlation between the chip flow angle and the size of burr. In general, two principles can be deduced: a larger burr is developed on the side over which the chip flows and the larger size of burr results from the larger chip flow angle on that side.

2. control of sideward burr formation is possible simply by adjusting the chip flow direction in rotary machining

Since the non-zero chip flow angle brings about

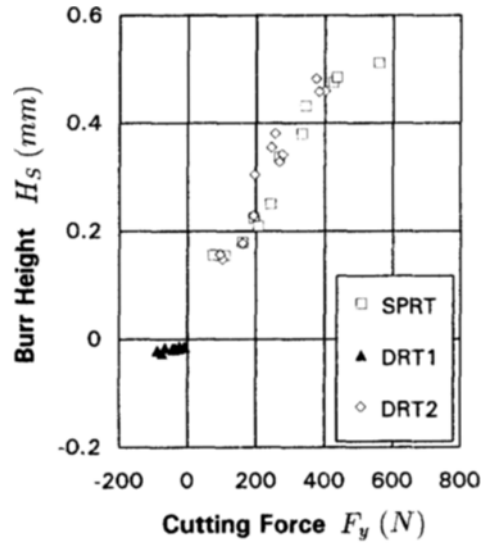

(a)

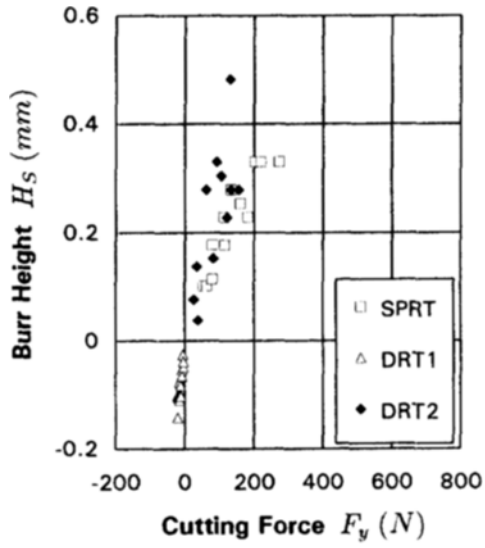

(b)

(**Fig. 9** Continued)

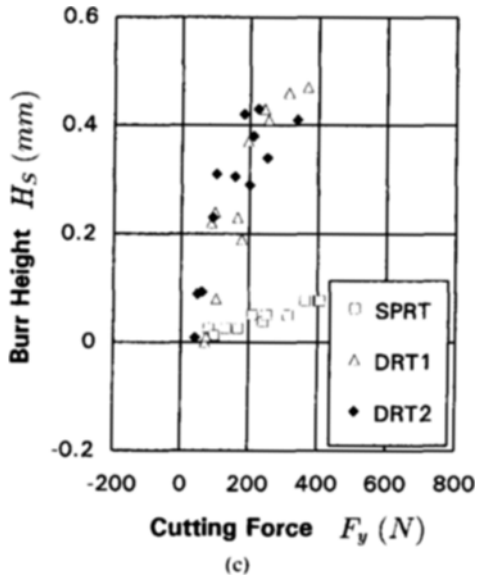

Fig. 9 Variation of H_S with F_y. Workpiece: Copper, (a); A11100, (b); A12024~T3, (c). Cutting conditions are same as in Fig. 7.

the force component in y direction in Fig. 6 (F_y), it is interesting to see how the size of burr is correlated with this force components. For example, Fig. 9 shows the experimental relationship between F_y and H_S obtained for various combinations of depth of cut, i_F and the tooling mechanism. Again, a linear relationship can be established between the two variables such that

$$H_S = C_3 F_y + C_4 \tag{6}$$

For small depth of cut, Poisson burr is produced by high pressure between the tool flank and the workpiece extruding material along the cutting edge axis (Gillespie and Blotter, 1967). Then, in order to investigate the pure effect of F_y on the sideward burr formation (denoted as H_{yo}), it is necessary to decompose the size of Poisson burr from H_S Since a linear relationship between the size of Poisson burr and F_x was established in Eq. (5), one can assume that

$$\begin{aligned} H_{yo} &= H_S - H_P \\ &= C_3 F_y - C_1 F_x + C_4 - C_2 \\ &= C_5 F_{yo} + C_6 \end{aligned} \tag{7}$$

where

$$F_{yo} = \frac{C_3 F_y - C_1 F_x}{C_5}$$

$$C_6 = C_4 - C_2 \tag{8}$$

The variation of H_{yo} with F_{yo} is seen in Fig. 10. Comparing Fig. 10 with Fig. 9, one can notice that formation of rollover burr was predominant in the experiments performed. It is also noted that the level of H_{yo} for copper and A1100 varies significantly with F_{yo} depending on the tooling

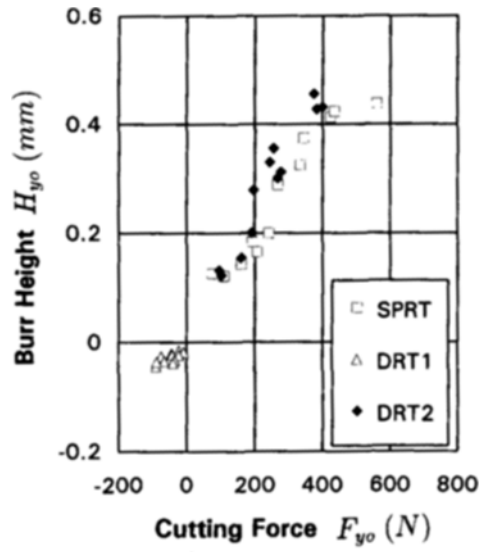

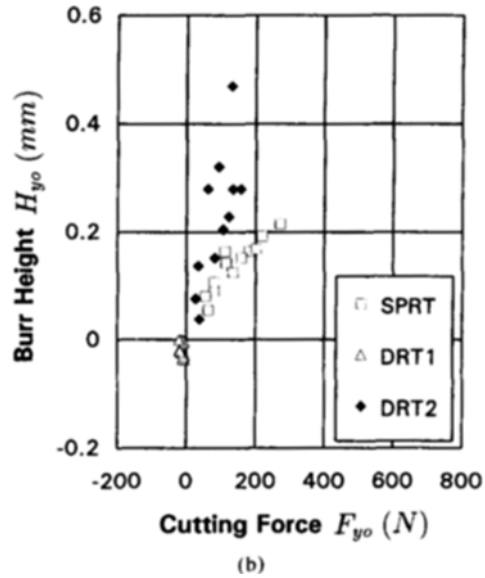

(**Fig. 10** Continued)

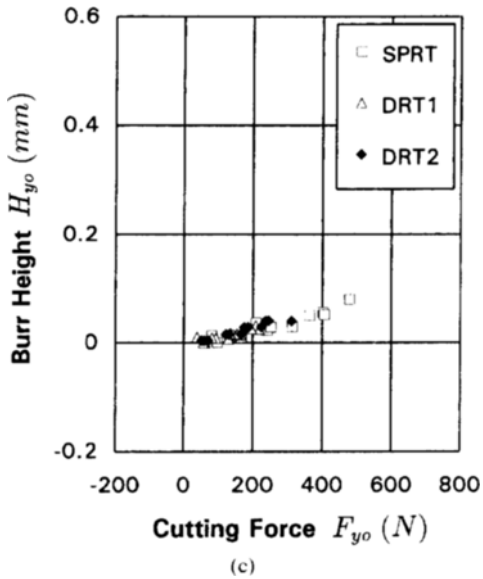

Fig. 10 Variation of H_s with F_{yo}. Workpiece: Copper, (a); Al1100, (b); Al2024~T3, (c) Cutting conditions are same as in Fig 7.

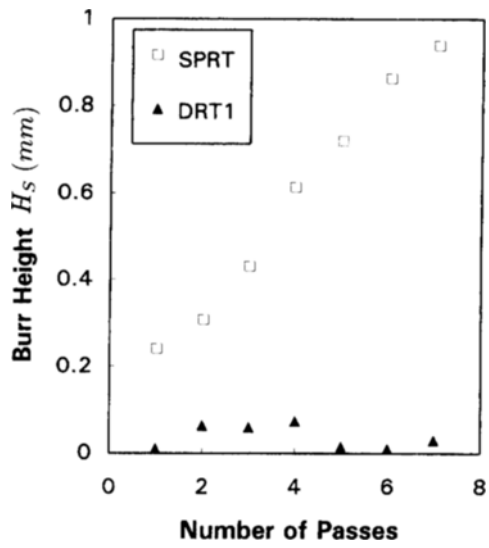

Fig. 11 Variation of accumulated H_s with number of passes in machining copper. Cutting conditions are same as in Fig.7.

mechanisms. A12024-T3 shows little dependence. This is because, as mentioned earlier, the ductile materials undergoes more plastic deformation than the brittle materials. Another piece of supporting evidence for this reasoning is that the sensitivity (slope) of H_{yo} to F_y is different for different materials and different tooling mechanisms. For example, chips of Al1100 and copper tend to triangulate with a SPRT as i_F increases, which results in higher cutting force components and larger size of burr. This explains the higher sensitivity of H_{yo} to F_{yo} for ductile materials. Interested readers should refer to (Choi and Choi, 1933) for more details about triangulation of chip in cutting with a SPRT. For DRT1, F_{yo} is either positive or negative for all materials but its magnitude is small, so is H_{yo} In this case, burr formation is similar to that of Poisson burr, hence Al1100 shows the steepest slope which coincides with results in Fig. 7. One thing to note at this point is that the intercept value K_2 in Eq. (4), which is usually neglected for investigation of chip formation process, was not subtracted from Eq. (7). It represents the plowing force at the tool flank face and the main squeezing effect in sideward burr formation is performed at the tool flank face (Pekelharing and Gieszen, 1971).

It was observed during the experiments with a DRT1 ($i_{eq} < -70^{\circ}$) that the chip tends to take the previously accumulated burr on the edge of the workpiece away from the workpiece with it. Even a heavily accumulated burr (H_S up to $1mm$) was completely removed in a single pass of DRT1. This point is illustrated in Fig. 11. With a SPRT, burr is accumulated continuously as the number of passes increases, whereas with a DRT1 the height of burr initially increases to a certain level and then the chip carries it away. Therefore, H_S shrinks to almost zero beyond this point.

5. Conclusions

Based on the experimental observations made in this study, the following conclusions can be drawn:

(1) The size of burr formed in rotary machining heavily depends on the tooling mechanism, e. g., SPRT, DRT1 or DRT2.

(2) The most significant factors that character-

ize the formation of sideward burr in rotary machining are the cutting force component in y direction, the direction of chip flow, and the magnitude of chip flow angle (η_c). These factors were found to have strong correlations with the size of burr (H_S). Minimization of this force component and proper control of chip flow can, therefore, lead to a minimum size of burr. This can be achieved simply by adjusting the rotary speed ratio, i_F and the tooling mechanism in rotary machining.

(3) DRT1 (DRT at high speed ratio in normal rotation) is found to be an effective means in minimizing the size of sideward burr or in completely removing the sideward burr formed on the edge portion of workpiece being machined.

References

Choi, G. H. 1990, "A Study on Rotary Machining," PhD Thesis, Department of Mechanical Engineering, University of California, Berkeley

Choi, G. H. and Choi, G. S., 1993, "Transient Chip Formation in Cutting with a Self-Propelled Rotary Tool," *Trans. KSME*, Vol. 17, No. 5, pp. 1041~1053

Gillespie, L. K. and Blotter, T., 1976, "The Formation and Properties of Machining Burrs," *J. Engr. for Industry, ASME*, Vol. 98, pp. 66~74

Ko, S. L., 1989, "Burr Formation and Fracture Mechanism at the Exit Stage of Metal Cutting," PhD Thesis, Department of Mechanical Engineering, University of California, Berkeley

Nakayama, K. and Arai, M., 1987, "Burr Formation in Metal Cutting," *Annals of the CIRP*, Vol. 36/1, pp. 33~36

Pekelharing, A. J. and Gieszen, C. A., 1971, "Material Side Flow in Finish Turning," *Annals of the CIRP*, Vol. 20/1, pp. 21~22

Shaw, M. C., Smith, P. A. and Cook, N. H., 1952, "The Rotary Cutting Tool," *Trans. ASME*, Vol. 74, Aug., pp. 1065~1076

Venuvinod, P. K. 1970, "Analysis of Rotary Cutting Tool," PhD Thesis, University of Manchester,

Venuvinod, P. K. and La u, W. S., 1981, "Some Investigations into Machining with Driven Rotary Tools," *J. Engr. for Industry, ASME*, Vol. 103, pp. 469~477